

# FLAT ROOF CLASSIFICATION AND LEAKS DETECTIONS BY DEEP LEARNING

*David Zahradník, Filip Roučka and Linda Karlovská*

*Czech Technical University in Prague, Faculty of Civil Engineering, Department of Geomatics,  
Thákurova 7, Praha 6, Czech Republic; david.zahradnik@fsv.cvut.cz*

## ABSTRACT

This paper presents an efficient and accurate method for detecting flat roof leaks using a combination of unmanned aerial vehicles (UAVs) and deep learning. The proposed method utilizes a DJI M300 drone equipped with RGB and thermal cameras to capture high-resolution images of the roof. These images are then processed to create orthomosaics and digital elevation models (DEMs). A deep learning model based on the U-NET architecture is then used to segment the roof into different classes, such as PVC foil, windows, and sidewalks. Finally, the damaged insulation is identified by analyzing the temperature distribution within the PVC foil segments. The proposed method has several advantages over traditional inspection methods. It is much faster and efficient. An UAV can collect images of a large roof in a matter of minutes, while traditional methods can take several days or weeks. The orthomosaics and temperature maps generated by the UAV are much more detailed than the images that can be collected by a human inspector. Third, the UAV-based system is safer. The UAV can collect images of the roof without the need for a human inspector to climb onto the roof, which can be dangerous. The results of this study show that the proposed method is an effective and accurate way to detect flat roof leaks. The deep learning model was able to achieve an overall accuracy of 95% in segmenting the roof into different classes. The method was also able to identify damaged insulation with a high degree of accuracy.

## KEYWORDS

Thermography, Remote sensing, CNN, U-NET, Flat roof leak detection, Deep learning

## INTRODUCTION

Flat roofs in large industrial halls are the weakest link in the whole building. A flat roof is characterized by its low pitch, which gives the advantage of covering a large area at a lower cost than pitched roofs. The flat roof has one major drawback in the form of slow rainwater drainage. Flat roofs can have a slope almost to the horizon, i.e. in the range of 0-1 degrees, which is often used on modern buildings or to create a roof terrace. Low pitch, which ranges between 1-5 degrees, is a common choice for commercial buildings and allows for a variety of uses such as solar panels or roof gardens. Roofs with a moderate pitch (5-10 degrees) are suitable for residential and commercial buildings and allow for relatively easy maintenance and efficient drainage. Due to the slow rate of rainwater runoff, great emphasis is placed on the design of flat roofs and their subsequent control according to the composition.

There are several compositions of flat roofs, and each plays a key role in providing stability, insulation and weather protection to this modern roof structure. We start with the roofing material, which is the first layer that forms the outer surface of the roof. This covering can be made from a variety of materials such as asphalt board, PVC sheeting, EPDM (ethylene propylene diene monomer rubber) rubber membranes, TPO (thermoplastic olefin) sheeting or concrete tiles, and is designed to resist weathering and provide an aesthetically pleasing appearance like on Figure 1.

This is followed by a waterproofing layer, which is key to keeping the roof dry. This layer prevents water from penetrating the structure and can be made of different waterproofing materials such as bitumen sheeting or liquid waterproofing. This is followed by insulation, which serves to maintain the interior temperature and ensure the energy efficiency of the building. Insulation materials include foam, mineral wool, expanded polystyrene (EPS) or extruded polystyrene (XPS). The drainage system, comprising the roof pitch and drainage elements such as gutters, downspouts and roof mats, is another important element. Its purpose is to quickly drain rainwater and prevent water from standing on the roof, which could cause failures. Security against wind and weather can be achieved by using a wind barrier.



*Fig. 1 – Example of typical flat roof*

Flat roofs covered with PVC membranes or even other membranes are susceptible to cracks, holes and other wear and tear caused by careless handling during construction, degradation from UV rays or others. Rainwater subsequently runs off through the hole into other layers of the roof composition. The water can remain in the waterproofing layer where it causes a reduction in the functionality of the thermal insulation in which the insulation becomes a conductor of heat. Water can seep through to the inside of the building and damage the interior and equipment of the building. An example of a flat roof leak is visible in Figure 2.

Regular inspection of flat roofs is key to addressing leaks effectively. Various methods exist for detecting holes in PVC foil roofing, including visual inspection, electropulse testing, needle testing, and smoke testing. These non-destructive techniques enable precise localization of holes in small areas, typically within a radius of about 0.5 meters. However, for larger roofs exceeding 10,000 square meters, employing these methods can become costly. An alternative solution for such extensive roofs involves thermography conducted by unmanned aerial vehicles (UAVs), offering efficient detection and assessment of leaks.

Thermography offers a non-invasive glimpse into the building's health, but accurate interpretation hinges on meticulous data acquisition. Surface emissivity, the culprit of varied thermal signatures even in identical materials, can be tamed through combined thermal camera and contact thermometer measurements. Reflected apparent temperature, another influential factor, is addressed by incorporating a reference object for subsequent corrections. Atmospheric attenuation, caused by air temperature and humidity, is easily mitigated by post-processing corrections based on weather station data. Finally, the camera-object distance, automatically embedded in modern thermograms, eliminates distance-related biases. By diligently accounting for these factors, thermography empowers researchers and professionals with reliable data to pinpoint heat loss,

thermal anomalies, and potential damage, paving the way for optimal building health and energy efficiency.



*Fig. 2 – Flat roof leak sample*

Thermal images captured by terrestrial thermal cameras require adjustments for perspective correction [1] and compensation for reflected longwave radiation from the Sun [2]. Despite their low resolution, thermal images can be processed using SfM (Structure from Motion) techniques [3]. Combining RGB images with thermal images enhances model detail [4], and aerial thermal imaging complements terrestrial coverage [5].

Detecting defects becomes challenging due to shadows, addressed either by capturing images under cloudy conditions or by segmenting thermal images for analysis [6]. Aerial thermal imaging, utilizing uncooled thermal cameras, suffers from vignetting nonuniformity, necessitating temperature calibration for accuracy [7]. Moreover, aerial thermography aids in calibrating building envelope models to meet energy efficiency standards [8-9].

The use of thermal cameras on drones has only recently begun. Lightweight thermal cameras had very low resolution and it was practically difficult to process the data by SfM. It was only about five years ago that improvements were made, the resolution of thermal cameras was increased and the software was adapted [10].

Thermography is an important tool in modern engineering and construction, allowing non-invasive detection and evaluation of defects in structures without compromising their integrity. To find a flat roof leaks, the total area of the roof must be recorded. It is therefore easier to use UAVs for data collection and subsequent processing of thermograms into orthomosaics than single thermograms. Thermograms that capture thermal distributions can be processed similarly to standard RGB images, except that they have a lower resolution. Professional thermal imaging cameras often offer a resolution of 640x512 px, which is significantly lower than standard RGB images. This limitation must be considered when photogrammetrically processing thermographic data [11-15].

Convolutional Neural Networks (CNNs) represent a class of deep learning architectures adept at tasks like image recognition and processing. Inspired by the human visual cortex, CNNs comprise layers designed to process input data hierarchically. At the outset, CNNs usually feature a convolutional layer tasked with feature extraction from the input image. This layer employs filters, small weight matrices, applied across different regions of the input, resulting in feature maps that encode detected features. Following the convolutional layer, a pooling layer is typically employed to downsample the feature maps, reducing their size while retaining essential information. The common max pooling operation selects the maximum value within specified regions of the feature map. This sequence of convolutional and pooling layers iterates through the network, progressively extracting more intricate features. Finally, a fully connected layer often concludes the CNN, responsible for classifying the input into predefined categories. [16] CNNs find wide-ranging applications, including land cover classification [17], tree species detection [18], and damage assessment following earthquakes [19].

U-Net stands out among convolutional neural network (CNN) architectures due to its specialization in pixel-level segmentation tasks, scheme of the network is in Figure 3. While traditional CNNs typically classify entire images, U-Net excels at identifying individual pixels belonging to specific classes within an image. This capability makes it particularly well-suited for tasks such as object detection, semantic segmentation, and instance segmentation. In drone orthophotos, U-Net can be trained to distinguish various elements such as buildings, roads, vegetation, water bodies, or even specific objects based on the application [21]. Through segmentation, this process effectively isolates these elements from the background, enabling detailed analysis and quantification. For instance, U-Net has been applied to scenarios such as detecting fallen trees after hurricanes or other disasters [22] and windthrow events [23]. Deep learning detection isn't limited to RGB or satellite data inputs. While RGB images are commonly used as the primary dataset, and most backbone models require RGB images, digital elevation models (DEMs) can also be utilized. Multi Directional Hillshade based on DEM data with three bands with 8 bits similar to RGB are suitable for Deep learning [24]. Another option is to leverage elevation data directly from the DEM, along with derived features such as slope (ranging from 0° to 90°) and terrain curvature [25]. These alternative data sources provide additional information that can enhance the capabilities of models like U-Net in various applications.

Deep Learning is also usable for Thermal abnormality detection. RGB images are used for the segmentation of visible buildings into walls, windows and doors and abnormality is localized by the temperature threshold of the anomaly area determined from the multimodal temperature distribution of the target domain [26].

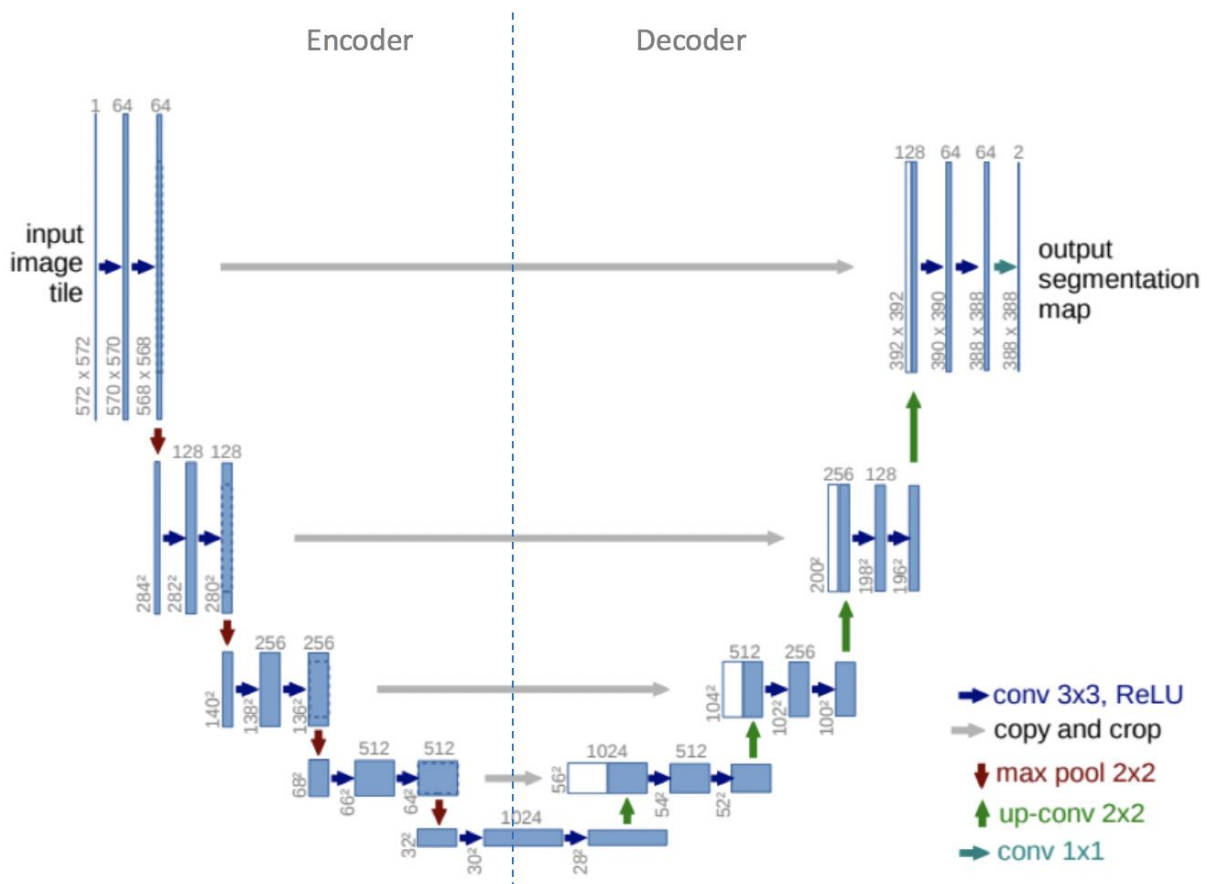


Fig. 3 – U-NET scheme [20]

## METHODS

### Testing data

Dozens of flat roofs were used for testing, flown from 2021 to 2024. The total area exceeds over 825,000 m<sup>2</sup> of flat roof area. Data collection was carried out on selected halls across the Czech Republic with implementation by NDN Tech company. The roofing on all flat roofs was made of PVC foil, on which flat roof leaks were searched. Roofs contain other categories like windows, walking paths, lightning rods and components, the percentage is in Figure 4.

Data for roof leak detection was collected using a DJI M300 drone equipped with a DJI P1 RGB camera and a DJI H20T thermal camera. RGB images were collected during the day to ensure good lighting conditions for the creation of a digital elevation model (DEM) and an RGB orthomosaic. Thermal images were collected after sunset to take advantage of the thermal contrast between the insulation and the surrounding environment.

High thermal contrast is essential for accurate leak detection. This contrast is most pronounced during the cooling and heating phases of the day when the insulation and the surrounding environment are at different temperatures.

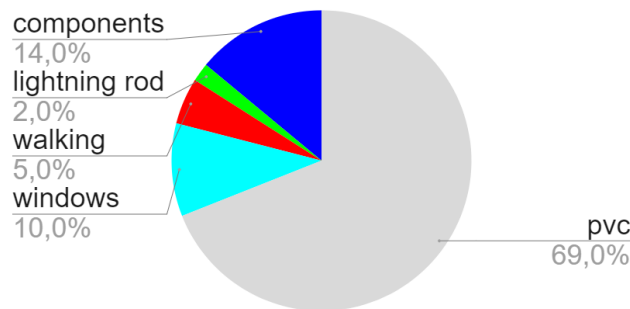


Fig. 4 – Diagram of the percentile of class on the roof

### Workflow of automatic flat roof leak detection

The full workflow consists of several steps based on image collection, preprocessing raw images, processing Ortomosaic and DEM in Agisoft Metashape, preprocessing raster data, training and applying the CNN model, raster segmentation and classification of a flat roof leak. The Workflow scheme is visible in Figure 5.

Data is collected by DJI M300 with DJI P1 and DJI H20T camera with automatic planning mission over a flat roof. All images have coordinates from the RTK module connected to the nearest GNSS permanent station. RGB images were captured during the day with good light conditions. TIR images were captured after sunset to eliminate reflected radiation and spot radiation emission with high contrast between damaged insulation and fine. Image specifications are in Table 1 below.

TIR images captured on UAV contain relative temperature and raw data. For absolute material temperature, TIR images must be calibrated by material emissivity, reflected radiation, atmospheric radiation, air temperature, humidity and distance from the object. Most elements are known from auxiliary measurements except material emissivity. Material emissivity is known from laboratory tests, but in real conditions, emissivity is far from the laboratory value. During the data acquisition method of determination, material emissivity and absolute material temperature were found as calibration of the thermograms. Calibration of the thermograms is performed using temperature calibration points. At the calibration points the absolute temperature is measured with a contact thermometer. For thermograms with a captured calibration point, the emissivity of the

material is determined retrospectively and applied to the rest of the thermograms in the TIR dataset. Thermal calibration points are selected on the PVC foil of the flat roof. The temperature of these points is measured before the UAV flies and after to control temperature drop. Points are signaled by an aluminium target to be visible on TIR images.

RGB images are processed in Adobe Lightroom from raw to jpg to correct exposure, fix highlights and pull shadows. The images are then processed in Agisoft Metashape to create DEM and RGB orthomosaics. Image coordinates sometimes contain the wrong position due to a lack of mobile signal when using GNSS correction. To avoid this problem, it is better to align the photo relative and after alignment apply georeferencing by image coordinates. Images with wrong coordinates contain higher position errors and fine georeferencing is prevented.

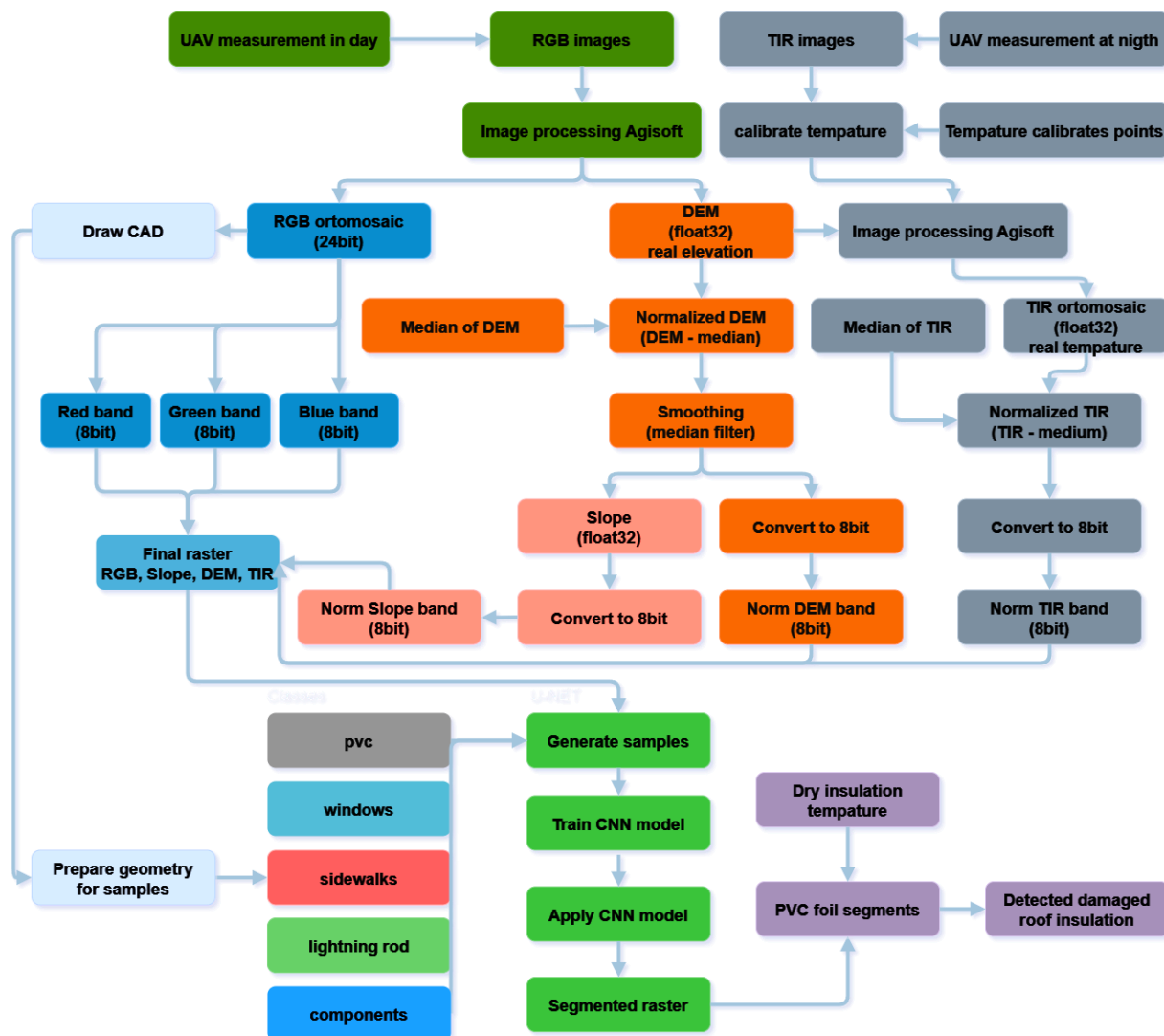


Fig. 5 – Process scheme

Processing of TIR images in Agisoft Metashape is done as RGB images except for DEM computation. Due to the low resolution of TIR images, it is better to use DEM from RGB images. Georeferencing with RTK coordinates allows the blending of RGB and TIR datasets without common control points. Ortho Mosaicing of the TIR dataset is based on DEM from the RGB

dataset. Results from image processing in Agisoft Metashape are RGB orthomosaic (24bit), DEM (32bit float), and TIR orthomosaic (32bit float).

*Tab. 1 - Methods of processing time*

	RGB images	TIR images
cameras	DJI P1	DJI H20T
resolution [px]	8192x5460	640x512
lens [mm] / Equival.	35	58
FOV [°]	63.5	40.6
time	day	sunset
above ground level (AGL) [m]	80	50
ground sample distance (GSD) [cm]	1	4.4
Overlap	80%, 60%	90%, 80%

Before training CNN (Convolutional Neural Network) model, rasters must be united into the same data type. Different data types are not allowed by the CNN model like 8bit vs. 32bit float. Most CNN models work with RGB data due to the most common sensor. Thermal data for the detection of flat roof leaks are also valuable information for classification by the CNN model. Objects on flat roofs are made from different materials with different emissivity and temperatures shown on thermograms in Figure 6. For example, the ventilation temperature on flat roofs is temperature-dependent on the cooling or heating process. The colour may be the same as PVC foil but the temperature is diametral different, this will help the CNN model to differentiate objects. Problems appear when each flat roof is inspected at a different time and season, and air condition and building operating temperatures are different. For purposes of the CNN model, data must be normalized by the median of TIR orthomosaic, which is the average temperature of PVC foil. Normalization excluded different temperatures across flat roof datasets.



*Fig. 6 – Example of TIR orthomosaic*

During the photogrammetry process in Agisoft MetaShape to achieve RGB and TIR orthomosaic DEM is created. DEM can extract useful information for the CNN model like altitude and slope. Altitude has the same problem as temperature, it is unique on each flat roof. Each building is built in a different area with some altitude. The usage of raw height from DEM for the CNN model will be not sufficient. Dem must be normalized by the median of DEM values, which is the height of a flat roof. The flat roof value on normalized DEM will be 0; other components will have different values. Some flat roofs have different levels, each level can be inspected for flat roof leaks. A flat roof level has a value other than 0 on normalized DEM and the CNN model can misclassify the level. The solution is to calculate slope based on DEM, but DEM by photogrammetry process may contain noise on PVC foils because of low contrast on RGB images and GSD. Due to the issue, DEM must be filtered to achieve smooth values Figure 7. For smoothing DEM used a median filter with a 3x3 kernel. After the smoothing slope can be calculated and the wrong values on PVC foil disappear, the comparison is visible in Figure 6.

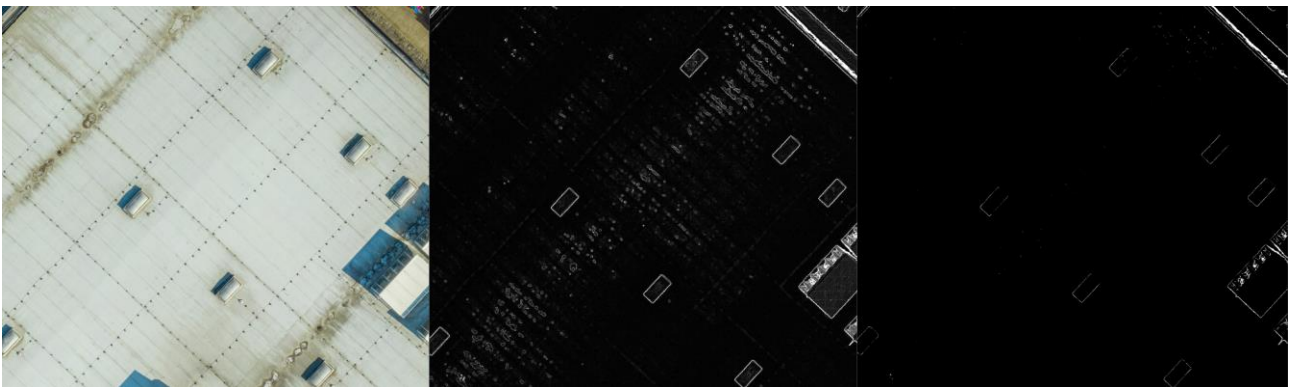


*Fig. 7 – RGB orthomosaic (left), Slope before DEM filtering (middle), Slope after DEM filtering (right)*

The RGBDTS raster used for creating samples for the U-NET model is composed of bands Red, Green, Blue, nDEM (normalized Digital Elevation Model), nTIR (normalized Thermal infrared) and Slope. All bands have the same 8-bit type for usage in the CNN model. For sample creation, CAD drawings are used for the first classification of flat roofs. CAD drawings were created as part of a job of flat roof inspection by company NDN tech. Computer aided design CAD drawings were converted into polygons representing each class of flat roof: PVC foil, windows, sidewalks, lightning rods and components.

### **Trimble eCognition - CNN approach**

Using the Vector-based segmentation in Trimble eCognition was then from the polygons created image objects. These image objects were then classified responding to the number and type of input classes. From these classified image objects were then created samples for the CNN. The type of samples was used in RAW format, sample count was 50 000 and the sample patch size was 32 pixels. Samples were made for each layer of RGB texture. The Convolutional Neural Network contained 2 hidden layers. The kernel of the first layer was set at 7 and the number of distinct feature maps was 12. The kernel of the second layer was set to 5. The CNN was trained with a 0.0006 learning rate, with 5000 training steps and 50 samples were used in each training step. After applying the CNN, heat maps of each class were created. The Values of heat maps represent probabilities of occurrence of each class.

The RGBDTS raster is used with OBIA segmentation to achieve segments most similar to real objects of flat roofs. Object-Based Image Analysis (OBIA) is a technique that moves beyond the traditional pixel-based analysis commonly used in remote sensing. Instead of treating individual

pixels as the smallest unit of analysis, OBIA groups pixels into meaningful objects or segments based on their spectral, spatial, and contextual characteristics (shape and compactness). This approach allows for a more accurate and context-aware interpretation of the data. Segments are classified into PVC foil, windows, sidewalks and other classes by heatmap from the CNN model. With classified PVC foil, it is possible to divide segments into damaged and fine insulation. Damaged insulation has a higher temperature compared to fine insulation. PVC foil segments are classified by the rule: IF temperature PVC foil exceeds 0 from nTIR class as a flat roof leak.

### ArcGIS - U-NET approach

The U-NET model's training chips were generated using 256x256 pixel tiles extracted from the RGBDTS raster data. Each tile contained polygons defining the different classes present in the scene. Training chips were in the "Classified Tiles" format.

The U-NET model underwent training with data augmentation techniques specified in Table 2. The training was conducted in batches of 8 samples for 20 epochs, with 10% of the data designated for validation purposes. A ResNet34 architecture served as the backbone for the deep learning model.

*Tab. 2 - Methods of processing time*

	Min	Max	Step
Rotate	0	360	10
Brightness	0.4	0.6	1
Contrast	0.7	1.5	1
Zoom	0.7	1.3	1

Flat roof leaks were extracted on segmented PVC foil at a higher temperature than the rest PVC foil.

## RESULTS

### Trimble eCognition - CNN - heatmaps

The application of a Convolutional Neural Network (CNN) within the eCognition software yielded unsatisfactory results. This can be attributed to several limitations. Each image chip could only receive a single class label, leading to misclassification when containing multiple classes within its boundaries. Smaller chip sizes might not capture sufficient textural information crucial for the accurate classification of flat roof elements. Introducing more than three distinct classes resulted in insufficient heatmap resolution for effective classification Figure 8.

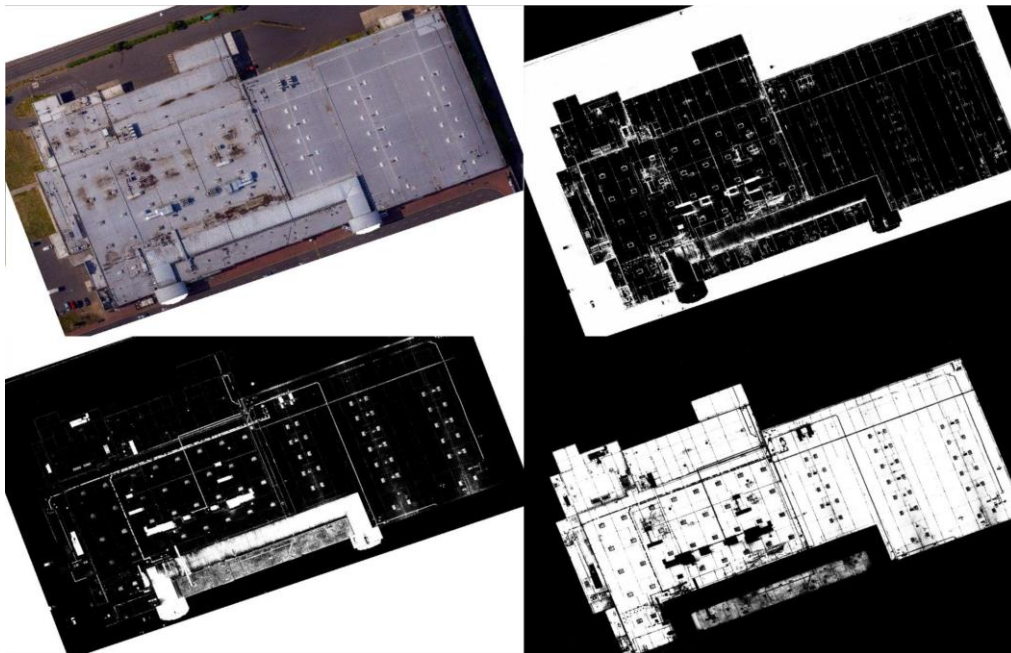


*Fig. 8 – Results from eCognition*

### ArcGIS - U-NET pixels segmentation

Leveraging U-NET within ArcGIS effectively segmented flat roof classes. Employing larger image chips successfully preserved textural information crucial for accurate classification. Notably, the Classified Tiles format proved advantageous by enabling the representation of multiple classes within a single chip, thereby mitigating mislabelling issues.

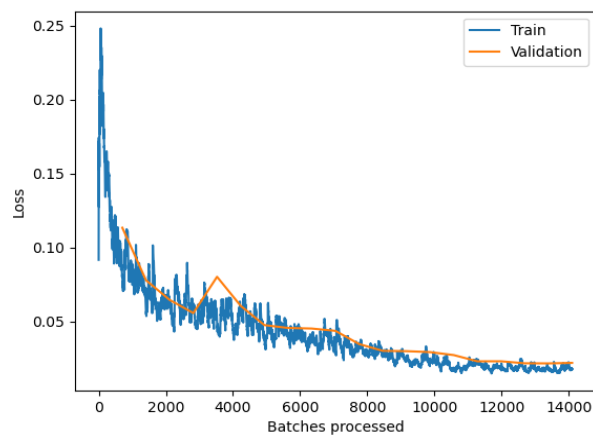


*Fig. 9 – Training loss*

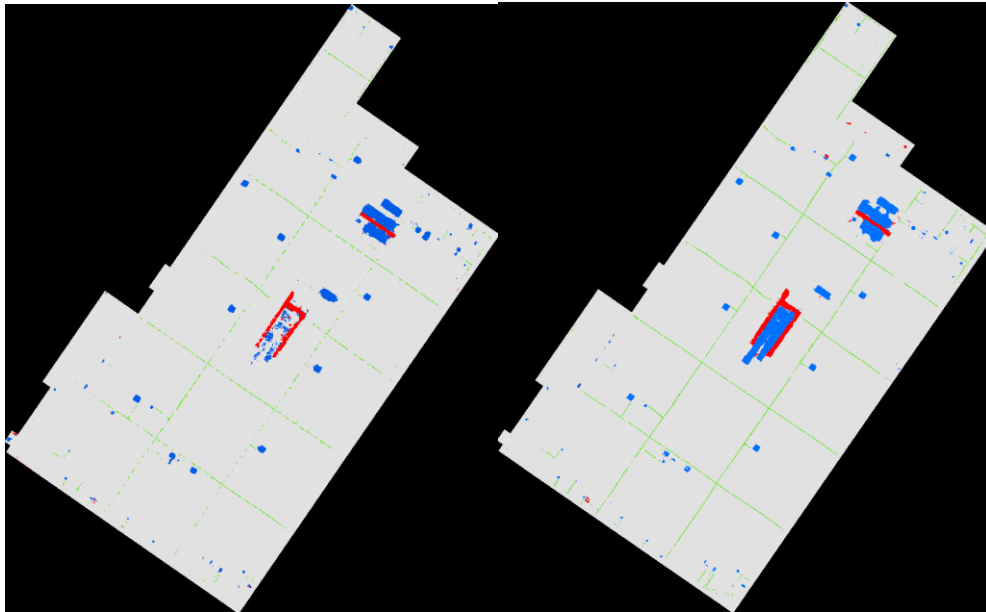


Fig. 10 – Results from ArcGIS

The efficacy of utilizing RGBDTS raster data was assessed against RGB raster data in terms of segmentation performance. Specifically, this evaluation focused on a flat roof scenario, employing identical network architectures, backbones, and other relevant parameters for both datasets. The results indicated superior segmentation outcomes when employing the RGBDTS raster compared to the RGB raster. Notably, there was no discernible difference in testing times between the two raster types, with both requiring equivalent time for one training epoch. Figure 10 visually represents the enhanced segmentation achieved across all three classes. This underscores the limitation of relying solely on colour information, particularly when distinguishing between classes with similar greyish hues. The resulting training results based on the RGBDTS raster are visible in Table 3 according to the evaluation equations (1-3) for deep learning.

$$Precision = \frac{TP}{TP+FP} \quad (1)$$

$$Recall = \frac{TP}{TP+FN} \quad (2)$$

$$F1 \text{ score} = \frac{TP}{TP + \frac{1}{2}(FP+FN)} \quad (3)$$

Tab. 3 - Methods processing time

	PVC	windows	lightning rod	components	walking
precision	0.994304	0.989148	0.926059	0.815632	0.980574
recall	0.995657	0.990409	0.937605	0.807025	0.952942
f1	0.994980	0.989778	0.931796	0.811306	0.966561

## CONCLUSION

This study successfully demonstrated a streamlined and precise approach to flat roof leak detection, merging the power of remote sensing data and deep learning. By leveraging a DJI M300 drone equipped with RGB and thermal cameras, we captured comprehensive roof data and processed it into orthomosaics and DEMs. The U-NET deep learning model excelled at segmenting the roof into distinct classes (PVC foil, windows, sidewalks), paving the way for leak identification. Damaged insulation was pinpointed by analyzing temperature variations within PVC foil segments, effectively revealing leaks.

This novel method surpasses traditional inspection methods in several key aspects. Firstly, it boasts remarkable speed and efficiency, allowing UAVs to capture large roof areas in minutes, compared to days or weeks required by conventional methods. Secondly, the UAV-based system delivers superior accuracy, generating highly detailed orthomosaics and temperature maps that far exceed the capabilities of human inspectors. Most importantly, it prioritizes safety by eliminating the need for inspectors to physically climb roofs, thereby mitigating potential dangers.

The achieved results are highly promising, showcasing an overall segmentation accuracy of 95% for the deep learning model and a high degree of success in pinpointing damaged insulation. This innovative approach holds immense potential to revolutionize flat roof inspections, offering significant advantages:

Inspections can be completed much faster, reducing time and resource expenditure. Detailed data acquisition and analysis lead to more precise leak detection and damage assessment. Eliminating the need for manual roof access minimizes risks for inspectors. Detailed roof condition information facilitates informed maintenance and repair decisions.

By integrating additional classes (attics, ventilation systems, drainage elements) and refining the deep learning model with more data, the system's capabilities can be further expanded. This paves the way for a future where UAV-based inspections become the norm, ensuring safer, more efficient, and cost-effective flat roof management.

## ACKNOWLEDGEMENTS

This work was supported by the Grant Agency of the Czech Technical University in Prague, grants SGS23/052/OHK1/1T/11.

## REFERENCES

- [1] Antón García, D., & Amaro Mellado, J. L. 2021. Engineering graphics for thermal assessment: 3D thermal data visualisation based on infrared thermography, GIS and 3D point cloud processing software. *Symmetry*, 13(2(335)), <https://doi.org/10.3390/sym13020335>
- [2] Acuña Paz y Miño, J., Duport, N., & Beckers, B. 2021. Pixel-by-pixel rectification of urban perspective thermography. *Remote Sensing of Environment*, 266, 112689, <https://doi.org/10.1016/j.rse.2021.112689>
- [3] Dlesk, A., Vach, K., and Holubec, P., 2018. Usage of Photogrammetric Processing of Thermal Images for Civil Engineers. (2018). *Int. Arch. Photogramm. Remote Sens. Spatial Inf. Sci.*, XLII-5, 99–103, <https://doi.org/10.5194/isprs-archives-XLII-5-99-2018>
- [4] Adamopoulos, E., Volinia, M., Giroto, M., & Rinaudo, F. 2020. Three-Dimensional Thermal Mapping from IRT Images for Rapid Architectural Heritage NDT. *Buildings*, 10(10):187, <https://doi.org/10.3390/buildings10100187>
- [5] Daffara C, Muradore R, Piccinelli N, Gaburro N, de Rubeis T, Ambrosini D. 2020. A Cost-Effective System for Aerial 3D Thermography of Buildings. *Journal of Imaging*. 6(8):76. <https://doi.org/10.3390/jimaging6080076>
- [6] Huang, Y., Shih, P., Hsu, K. T., & Chiang, C. 2020. To identify the defects illustrated on building facades by employing infrared thermography under shadow. *NDT & E International*. <https://doi.org/10.1016/j.ndteint.2020.102240>

- [7] Yuan, W., & Hua, W. 2022. A Case Study of Vignetting Nonuniformity in UAV-Based Uncooled Thermal Cameras. *Drones*, 6(12), 394.
- [8] Bayomi, N., Nagpal, S., Rakha, T.,, Fernandez,J.E. 2021. Building envelope modeling calibration using aerial thermography, *Energy and Buildings*, Volume 233, 110648, ISSN 0378-7788, <https://doi.org/10.1016/j.enbuild.2020.110648>.
- [9] Rakha, T., El Masri,Y., Chen, K., Panagoulia, E., De Wilde, P. 2021. Building envelope anomaly characterization and simulation using drone time-lapse thermography, *Energy and Buildings*, 111754, ISSN 0378-7788, <https://doi.org/10.1016/j.enbuild.2021.111754>
- [10] Straková, H.; Šedina, J.; Bila, Z. Monitoring of Heaps Using Various Technologies. 2015. *Civil Engineering Journal*. 2015/ 2 ISSN 1805-2576. <https://doi.org/10.14311/CEJ.2015.02.0011>
- [11] Dlesk, A., Vach, K., & Pavelka, K. 2022. Photogrammetric Co-Processing of Thermal Infrared Images and RGB Images. *Sensors*. <https://doi.org/10.3390/s22041655>
- [12] Dlesk A, Vach K, Pavelka K. 2021. Transformations in the Photogrammetric Co-Processing of Thermal Infrared Images and RGB Images, *Sensors*. 2021; 21(15):5061. <https://doi.org/10.3390/s21155061>
- [13] Motayyeb, S., Samadzedegan, F., Javan, F. D., & Hosseinpour, H. 2023. Fusion of UAV-based infrared and visible images for thermal leakage map generation of building facades. *Heliyon*, 9(3)
- [14] Stokowiec, K., & Sobura, S. 2022. Hand-held and UAV camera comparison in building thermal inspection process. In *Journal of Physics: Conference Series* (Vol. 2339, No. 1, p. 012017). IOP Publishing.
- [15] Kuo, C. F. J., Chen, S. H., & Huang, C. Y. 2023. Automatic detection, classification and localization of defects in large photovoltaic plants using unmanned aerial vehicles (UAV) based infrared (IR) and RGB imaging. *Energy Conversion and Management*, 276, 116495.
- [16] Osco, L. P., Marcato, J., Ramos, A. P. M., De Castro Jorge, L. A., Fatholahi, S. N., De Andrade Silva, J., Matsubara, E. T., Pistori, H., Gonçalves, W. N., & Li, J. 2021. *A review on deep learning in UAV remote sensing*. *International Journal of Applied Earth Observation and Geoinformation*. <https://doi.org/10.1016/j.jag.2021.102456>
- [17] Naushad, R., Kaur, T., & Ghaderpour, E. 2021. Deep Transfer Learning for Land Use and Land Cover Classification: A Comparative Study. *Sensors*. <https://doi.org/10.3390/s21238083>
- [18] Natesan, S., Armenakis, C., & Vepakomma, U. 2019. *Resnet-Based Tree Species Classification Using UAV Images*. (2019). *The International Archives of the Photogrammetry, Remote Sensing and Spatial Information Sciences*. <https://doi.org/10.5194/isprs-archives-xlii-2-w13-475-2019>
- [19] Yi-Jun, L., Mohammadi, M. E., & Wood, R. L. 2020. Deep Learning Classification of 2D Orthomosaic Images and 3D Point Clouds for Post-Event Structural Damage Assessment. *Drones*. <https://doi.org/10.3390/drones4020024>
- [20] How U-net works? | ArcGIS API for Python. 2024. <https://developers.arcgis.com/python/guide/how-unet-works/>
- [21] Reachsumit (2024). GitHub - reachsumit/deep-unet-for-satellite-image-segmentation: Satellite Imagery Feature Detection with SpaceNet dataset using deep UNet. GitHub. <https://github.com/reachsumit/deep-unet-for-satellite-image-segmentation>
- [22] Reder, S., Mund, J., Albert, N. G., Waßermann, L., & Miranda, L. 2021. Detection of Windthrown Tree Stems on UAV-Orthomosaics Using U-Net Convolutional Networks. *Remote Sensing*. <https://doi.org/10.3390/rs14010075>
- [23] Kislov, D. E., & Korznikov, K. A.2020. Automatic Windthrow Detection Using Very-High-Resolution Satellite Imagery and Deep Learning. *Remote Sensing*. <https://doi.org/10.3390/rs12071145>
- [24] Satari, R., Kazimi, B., & Sester, M. 2021. Extraction of linear structures from digital terrain models using deep learning. *AGILE: GIScience Series*. <https://doi.org/10.5194/agile-giss-2-11-2021>
- [25] A Deep Learning Model for Identifying Mountain Summits in Digital Elevation Model Data. 2018. *IEEE Conference Publication | IEEE Xplore*. <https://ieeexplore.ieee.org/stamp/stamp.jsp?tp=&arnumber=8527481>
- [26] Park, G., Lee, M., Jang, H. I., & Kim, C. 2021. Thermal anomaly detection in walls via CNN-based segmentation. *Automation in Construction*. <https://doi.org/10.1016/j.autcon.2021.103627>